Development, Demonstration, and Control of a Testbed for Multiterminal HVDC System

Yalong Li, *Student Member, IEEE*, Xiaojie Shi, *Student Member, IEEE*, Bo Liu, *Student Member, IEEE*, Wanjun Lei, *Member, IEEE*, Fred Wang, *Fellow, IEEE*, and Leon M. Tolbert, *Fellow, IEEE*

***Abstract*—This paper presents the development of a scaled four-terminal high-voltage direct current (HVDC) testbed, including hardware structure, communication architecture, and different control schemes. The developed testbed is capable of emulating typical operation scenarios including system start-up, power variation, line contingency, and converter station failure. Some unique scenarios are also developed and demonstrated, such as online control mode transition and station re-commission. In particular, a dc line current control is proposed, through the regulation of a converter station at one terminal. By controlling a dc line current to zero, the transmission line can be opened by using relatively low-cost HVDC disconnects with low current interrupting capability, instead of the more expensive dc circuit breaker. Utilizing the dc line current control, an automatic line current limiting scheme is developed. When a dc line is overloaded, the line current control will be automatically activated to regulate current within the allowable maximum value.**

***Index Terms*—HVDC, multiterminal, multiterminal HVDC (MTDC), testbed.**

I. Introduction

DRIVEN by the increased penetration of remote renewable energy [1] and recent development of converter technology, especially the modular multilevel converter (MMC), interest in voltage source converter based high-voltage direct current (VSC HVDC) transmission has grown rapidly during the past decade [2]–[4]. The maximum dc voltage and power rating of commercial VSC HVDC systems have reached $\pm$320 kV and 2000 MW and are still increasing [5]. Compared to the traditional line-commutated converter, VSC can easily realize the power reversal through dc current polarity change, without the need to reverse the dc voltage polarity. Therefore, VSC HVDC is suitable to build a dc system with more than two converter stations, i.e., multiterminal HVDC (MTDC). Even though most existing HVDC systems are point-to-point and only a few MTDC projects have been installed, interest in MTDC or even more complicated dc grids has continued to grow. The benefits of MTDC include better use of transmission infrastructure and higher transmission flexibility and reliability. In the HVDC grid feasibility study by CIGRE [6], the economic benefit and technical feasibility of MTDC or HVDC grids are evaluated. Another economic assessment between the point-to-point HVDC and VSC MTDC was conducted in [7]. It was concluded that there is no clear preference between these two options before 2020, due to the need of expensive dc circuit breaker for the multiterminal system. However, the dc circuit breaker cost is expected to decrease in the future, as many manufacturers are involved in developing the new hybrid dc circuit breaker [8], [9], which brings more opportunities for VSC MTDC. However, there are also several unresolved issues and many ongoing activities, including dc fault protection, power flow control, system modeling [10], dc/dc converters, and grid codes [11].

Until now, the Nanao 3-terminal [12] (commissioned in 2013) and Zhoushan 5-terminal [13] (commissioned in 2014) in China are the only two VSC MTDC projects in the world. Little operation experience has been published, and many practical system control and protection issues still remain. Therefore, a number of scaled VSC MTDC testbeds were developed and reported in [15]–[18], with four or five terminals. A testbed is a valuable platform for control and protection development and is usually the technology pioneer for developing commercial projects. This paper presents the design and development of a four-terminal VSC HVDC testbed, with a dc ring topology. The two commercial projects and most other testbeds adopt the simplest radial topology of the dc system. However, meshed topology is getting more consideration due to its enhanced transmission reliability and flexibility; as the basic form of the meshed network, the ring connection or topology should become more common for future dc grids [19]. The five-terminal mock-up in [16] is the only other reported testbed forming a dc ring among three terminals, but only limited scenarios are emulated. Particularly, the station online recommission and mode transition have not been demonstrated in any other projects or testbeds before.

In the developed four-terminal testbed presented in this paper, the typical VSC MTDC operation scenarios are emulated and corresponding test results are presented. In addition, a dc line current control is proposed with the capability to regulate dc line current through station control. One benefit of this control

Manuscript received April 12, 2016; revised July 25, 2016 and October 5, 2016; accepted October 6, 2016. Date of publication October 21, 2016; date of current version March 24, 2017. This work was supported primarily by the Engineering Research Center Program of the National Science Foundation and the Department of Energy under NSF Award Number EEC-1041877 and the CURENT Industry Partnership Program. Recommended for publication by Associate Editor J. Liu.

Y. Li, X. Shi, B. Liu, F. Wang, and L. M. Tolbert are with the Department of Electrical Engineering and Computer Science, The University of Tennessee, Knoxville, TN 37996-2250 USA (e-mail: yli81@utk.edu; xshi5@utk.edu; bliu16@utk.edu; fred.wang@utk.edu; tolbert@utk.edu).

W. Lei is with the Department of Industry Automation, Xi'an Jiaotong University, Xi'an 710049, China (e-mail: leiwanjun@mail.xjtu.edu.cn).

Color versions of one or more of the figures in this paper are available online at http://ieeexplore.ieee.org.

Digital Object Identifier 10.1109/TPEL.2016.2620167

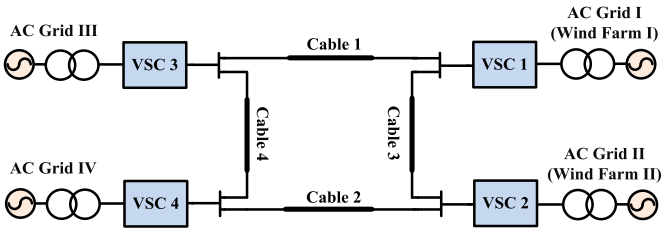

Fig. 1. Circuit diagram of the proposed four-terminal HVDC system.

Fig. 2. Proposed hypothetical system corresponding to Cape Wind Project in Northeast Power Coordinating Council system.

is to allow the use of a dc disconnect for online dc line trip. By controlling the line current to near zero, the dc disconnect with very low current breaking capability is able to trip a line without the need to de-energize the entire dc system, which is a less expensive solution compared to a dc circuit breaker. Based on this control, a dc line current limiting function is further proposed. It helps to prevent dc line overloading, as the line current control will automatically be activated once the line is overloaded and will regulate the current within the maximum allowable value.

II. Testbed Description

A. System Configuration and Parameters

Fig. 1 shows the circuit diagram of the proposed four-terminal HVDC system with a dc ring topology. Without loss of generality, an application scenario is considered in this paper that uses the four-terminal HVDC to integrate two offshore wind farms to two onshore ac grids. The proposed testbed can correspond to the hypothetical MTDC system transferring power from two wind farms in Cape Cod Bay area to two onshore load centers in Massachusetts (USA) and Connecticut (USA), as shown in Fig. 2. The system contains four power converter stations and four transmission cables, forming a dc ring network.

The detailed parameters of the proposed system are shown in Table I. The wind farm power ratings are roughly corresponding to the Cape Wind project [20]. From the geographical point of view, cables 1–3 cross both land and sea. But for simplicity, cables 1 and 4 are assumed as land cables only, and cables 2 and 3 are submarine cables.

TABLE I
Parameters of the Hypothetical System

Description	AC Grid I	AC Grid II	AC Grid III	AC Grid IV
DC voltage	±150 kV	±150 kV	±150 kV	±150 kV
AC voltage	33 kV	33 kV	345 kV	115 kV
Active power	250 MW	200 MW	250 MW	200 MW
Reactive power	–	–	150 Mvar	100 Mvar
Transformer ratio	33 kV/161 kV	33 kV/161 kV	345 kV/161 kV	115 kV/161 kV
	Cable 1	Cable 2	Cable 3	Cable 4
Type, Length	Land 100 km	Submarine 70 km	Submarine 60 km	Land 100 km

Fig. 3. Photograph of the MTDC testbed.

TABLE II
Parameters of the MTDC Testbed

Description	Values	Description	Values
DC voltage	400 V	Power rating of VSC 1,3	5 kW
AC voltage (rms)	208 V	Power rating of VSC 2,4	4 kW
Transformer	208 Yn/208 Δ	AC reactor of VSC 1,3	3.2 mH
DC-link capacitance	1.35 mF	AC reactor of VSC 2,4	4 mH
Cable 1 resistance, inductance	0.2 Ω 2.5 mH	Cable 2 resistance, inductance	0.15 Ω 2.5 mH
Cable 3 resistance, inductance	0.5 Ω 2.5 mH	Cable 4 resistance, inductance	1 Ω 3.5 mH

B. Testbed Description

A testbed is developed based on the proposed system as shown in Fig. 3, and Table II lists the main parameters of the testbed. The 208 $V_{\rm ac}$ grid in the lab is used, and the rated power of the larger stations (VSCs 1 and 3) in the testbed are chosen as 5 kW. Therefore, the testbed is power scaled with a factor of 1/50 000 from the hypothetical system, and the scaling principle for other electrical parameters is to maintain the per-unit values. The detailed circuit diagram in each downscaled power station is shown in Fig. 4. As the testbed is mainly developed for system control demonstration, the converter topology has little impact on the system operation. Therefore, two-level VSCs are used instead of the state-of-the-art MMCs without loss of

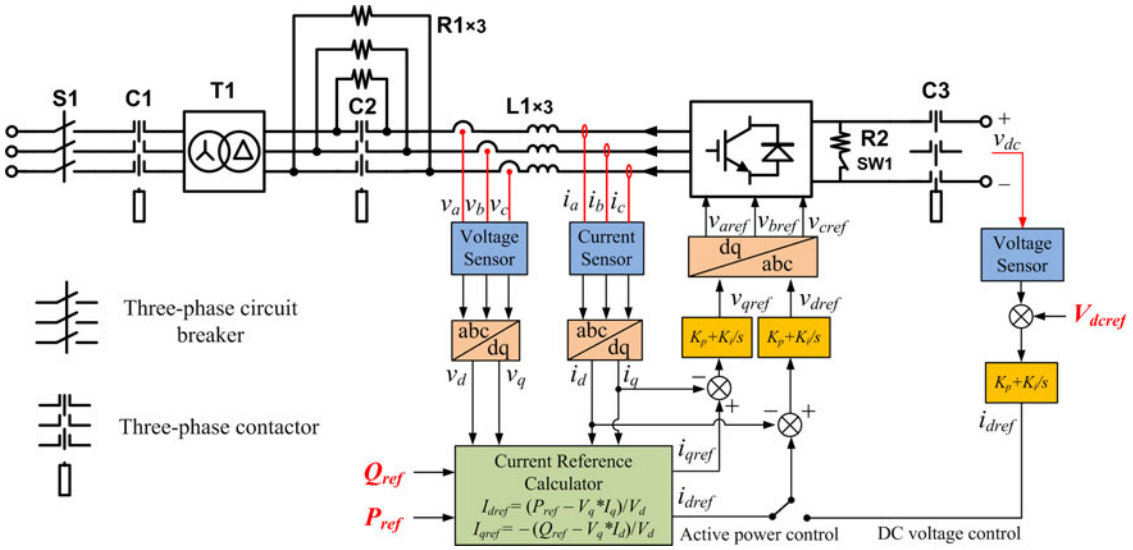

Fig. 4. Circuit diagram and control schemes of the downscaled power station.

generality. The converter ac terminal is connected to a stiff grid through interfacing reactors, a precharge circuit, and an Yn/Δ line-frequency transformer. Additional reactors can be series connected to emulate a weak ac grid connection. On the dc side, the converter connects to the joint of two cables and a discharge resistor is paralleled for dc capacitor energy dissipation after station shut down. The dc cable is emulated by discrete passive elements, according to the lumped π model [21]. The equivalent inductance, capacitance, and resistance of each cable in the hypothetical system are obtained from ABB land and submarine cable data [4] and then scaled for the testbed system. Only equivalent resistors and inductors are installed in the testbed, as the capacitors can be considered as combined into the dc link capacitor of each station.

1) Converter Control: The converter is digitally controlled, using the Texas Instrument DSP TMS320F28335 as the controller. The converter control schemes are shown in Fig. 4 as well, with inner current loop and outer dc voltage/active power and reactive power control loops. AC voltage and frequency control are not implemented as the converter is connected to a stiff ac grid. So each converter can either operate at dc voltage and reactive power control mode (Vdc/Q), or active power and reactive power control mode (P/Q).

2) Coordinated DC Voltage Control: DC voltage control is a main objective and challenge in dc systems, similar to controlling the frequency in ac systems. An essential requirement is that at any time (including contingencies), the system should have at least one station participating in the dc voltage control. For instance, if a station responsible for dc voltage control fails, another station in the system has to take over the dc voltage control responsibility automatically, without the need for communication. Many coordinated dc voltage control schemes have been introduced in the literature. Voltage margin [22] and voltage droop [23] are the two most popular ones, and many other schemes are also based on them. These two methods are both

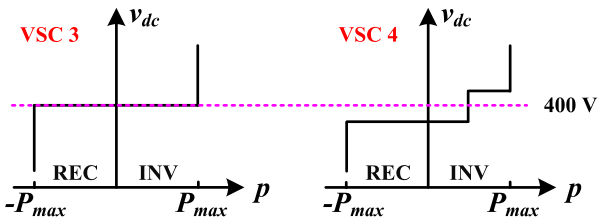

Fig. 5. $V_{\mathrm{dc}}-P$ characteristic curve for voltage margin control.

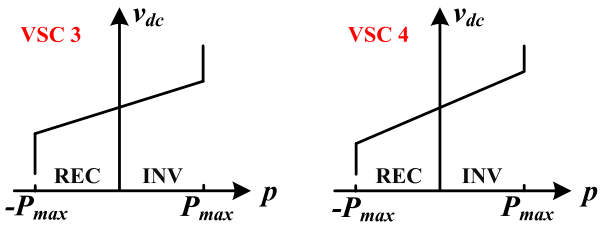

Fig. 6. $V_{\mathrm{dc}}-P$ characteristic curve for voltage droop control.

implemented in the testbed. Fig. 5 shows the $V_{\mathrm{dc}}-P$ characteristic curves of the two onshore converters (VSC 3 and 4) for voltage margin control. According to the curves, VSC 3 normally controls dc voltage and VSC 4 operates at P control mode. If for some reason such as a fault, VSC 3 loses the dc voltage control capability, the dc voltage will either increase or decrease until it reaches the voltage margin of VSC 4. After that, VSC 4 changes to dc voltage regulating mode. Therefore, the voltage margin control increases the system robustness in dealing with station outage.

Fig. 6 shows the $V_{\mathrm{dc}}-P$ characteristic curves for voltage droop control. There is no longer a constant dc voltage or active power reference. Instead, the dc voltage reference is online calculated by a function of the real-time active power, which is the $V_{\mathrm{dc}}-P$ droop control; or otherwise, the active power

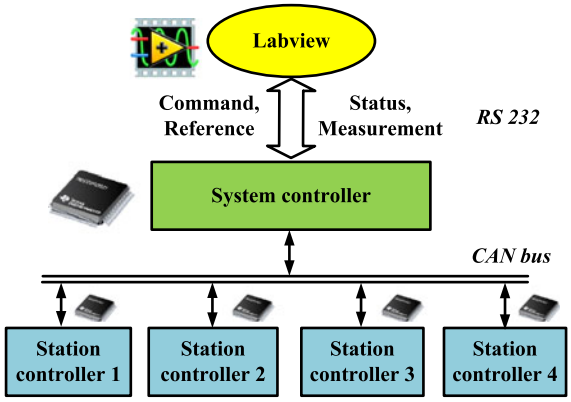

Fig. 7. Communication architecture of the MTDC testbed.

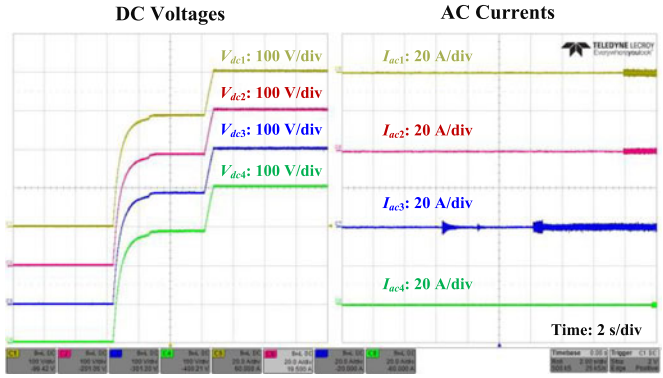

Fig. 8. Waveforms of system start-up.

reference is calculated based on dc voltage, that is $P - V_{\rm dc}$ droop control. With the droop control, both VSC 3 and 4 participate in the dc voltage control, and if one station fails, the other station can still maintain the dc voltage control. Even though only two terminals are shown here as an example, both the voltage margin and droop control can be used for more than two terminals.

3) Communication: In a real system, a system-level controller is usually needed beyond the station-level controller, responsible for command assignment (e.g., station start, stop, reset commands) and sending control references to each station (e.g., dc voltage, active power, reactive power reference). In the testbed, the system-level controller is fulfilled by another DSP, and a human interface communicating to the system-level controller is built using NI LabVIEW.

Fig. 7 shows the communication architecture in the testbed. The communication between computer (LabVIEW interface) and system-level controller is realized through RS232, and the system-level controller communicates with station-level controllers through a CAN bus in the DSP. Even though the communication speeds for both the serial and CAN bus in the testbed can be high, the data refresh frequencies for both of them are set slow at 10 Hz, to reflect the slow communication in most real grid applications.

The LabVIEW interface sends the commands and control references to the system controller, and then the system controller dispatches the data to each station. At the same time, each station gathers data, such as station status and some important measurements and sends them to the system controller. The system controller will package the data and send to Labview for real-time monitoring.

III. Operation Scenario Emulation

One main purpose in developing the testbed is to understand the operation and control of the MTDC system. Therefore, the developed testbed should be capable of emulating the typical MTDC operation scenarios and demonstrating different control schemes. In addition, several unique operation scenarios are also emulated, which have not been presented in any other testbeds but could be necessary in the real system. The emulated scenarios include:

1) system start-up;
2) station online recommission;
3) station power variation;
4) station online mode transition; and
5) station outage.

The labeling of traces in the waveforms is declared here: $V_{\rm dc}$, $I_{\rm dc}$, and $I_{\rm ac}$ represent the dc voltage, dc current and ac current, all at the converter terminals. The number in the subscript indicates which converter it belongs to, e.g. $V_{\rm dc1}$ represents the dc voltage of VSC 1. Also, the positive active power is defined as power injecting from dc to ac.

A. System Start-Up

The whole system may be shut down due to some severe faults. After the fault is cleared, the MTDC system needs to restart quickly and safely. To emulate this scenario, the start-up procedure in the testbed is as follows:

1) Make sure all four cables are connected and close the dc side contactors C3 (see Fig. 4) of all four stations.

2) Close the ac side contactor C1 of VSC 3, and the dc voltage is built up by a diode rectifier through precharge resistors.

3) Bypass the precharge resistor by closing C2 and enable the dc voltage control of VSC 3. The dc voltage is then ramped to the rated value.

4) Close C2 and C3 in the other stations and start the converters in P/Q mode.

This start-up procedure charges the dc-link capacitors of all four stations and dc cables at the same time. It avoids the high inrush current for energizing the dc cables separately. The waveform during start-up is shown in Fig. 8. The current ripples that appear during the last 2 s in VSC 1, 2, and 4 are due to deblocking pulse width modulation of those converters during the start-up procedure.

B. System Online Recommission

If a station is shut down due to fault or maintenance purpose, the remaining system should operate continuously. After repair or maintenance, the station should recommission online and

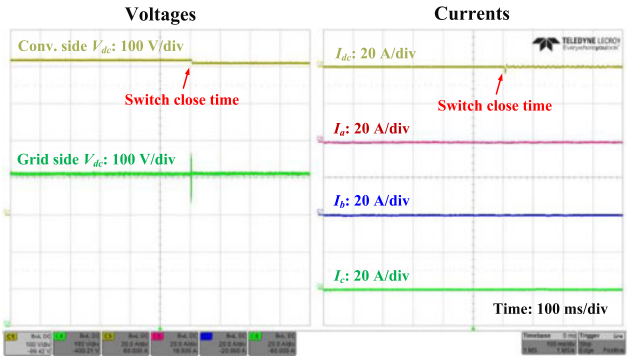

Fig. 9. Waveforms of station recommission with method I.

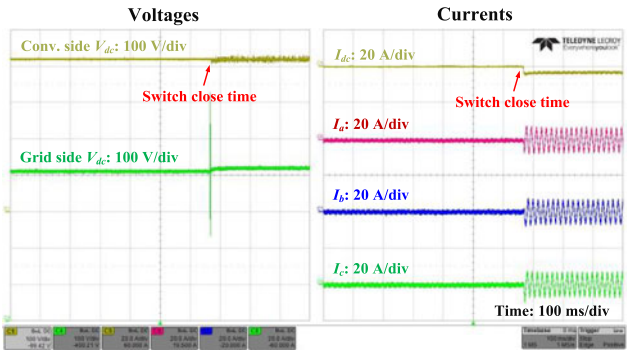

Fig. 10. Waveforms of station recommission with method II.

not require the shutdown of the whole system. In [24], the recommission method (method I) is to first build up the station dc voltage, and then close the dc switch while blocking the converter. The difficulty of this method is that the high-voltage dc switch usually takes a long time to close (approximately 10 s), which may cause a certain dc voltage decrease due to the dc-link capacitor discharge. Therefore, there is a voltage difference between the two sides of the dc switch when it is actually closed, and this generates a surge current. In [24], the voltage decay during the switch actuation delay time is estimated and the station dc voltage is charged to the grid side dc voltage plus the expected voltage decay.

However, it is not easy to estimate the voltage decay, as the delay time is not always the same and more importantly the dc voltage discharge rate is difficult to calculate. An alternative recommission method (method II) is not to block the converter, and to maintain dc voltage regulation while closing the dc switch. It avoids the need to estimate the voltage decay, but the converter devices become vulnerable during the recommission. Even though the station dc voltage is controlled equal to the grid side dc voltage, surge current may still occur and flows through the converter devices due to possible measurement or control error.

Both methods have been tested, and the test results are shown in Figs. 9 and 10. As the installed low voltage dc contactor closes much faster than the high-voltage counterpart, the voltage decay is thus small. To emulate the inaccuracy of the voltage decay estimation for method I, the station dc voltage is charged to

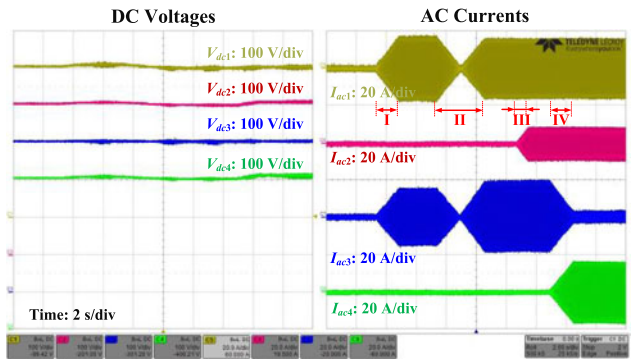

Fig. 11. Waveforms of station power variation with margin control.

2% higher than the grid side dc voltage. As for comparison, this 2% error is also applied for method II to account for the measurement and control error. As shown in the figures, the grid side dc voltage has a voltage spike when the switch is closed for both methods. This is mainly caused by the mechanical switch contact bounce, which should be alleviated due to the arc generation in real case at high voltage.

As shown in Fig. 9, there is no ac current during the recommission process as the converter is blocked. But dc current has a spike, small here but can become larger depending on the voltage difference between the two sides of the dc contactor. In Fig. 10, both ac and dc currents have a nearly step change. This is because the system power flow is changed after station recommission. The post recommission ac and dc inrush currents are acceptable in this test condition, but it changes with the voltage difference between the two sides of the dc switch and the cable resistance. Typically, the measurement and control errors are relatively small (2% assumption is already conservative [25]). The cable resistance can be very different due to the transmission distance variation. A large inrush current could still be generated, for example, in a system with much reduced cable resistance. However, because the inrush current is caused by the change of operating point, the voltage margin control can change the converter operating modes if the inrush current hits the maximum ac current limit to protect the converters. However, this could also be a potential disadvantage of method II, as it could introduce a large disturbance to the system.

The test results comparison shows that method I is a safer option, but more complicated as well. Method II on the contrary is simpler and the risk to converter power devices can be prevented by the voltage margin control. One of the disadvantages is that it may cause a large power disturbance.

C. Station Power Variation

Station power variation is one of the most typical scenarios of MTDC operation, especially for connecting an offshore wind farm, where the generated power varies all the time. Both dc voltage margin and droop control are tested. The waveforms are shown in Figs. 11 and 12, respectively.

1) Voltage Margin Control: VSC 3 operates at $V_{\rm dc}/Q$ mode and VSC 1, 2, 4 operate at P/Q mode. The tested transients include:

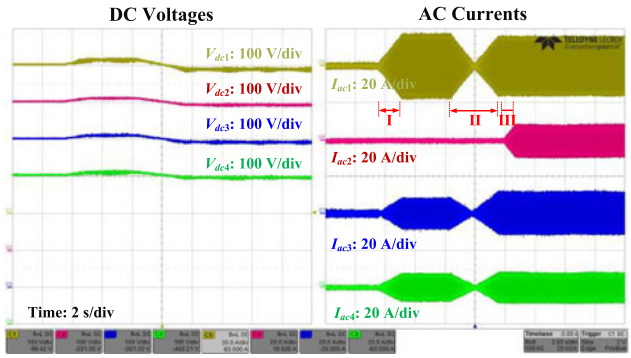

Fig. 12. Waveforms of station power variation with droop control.

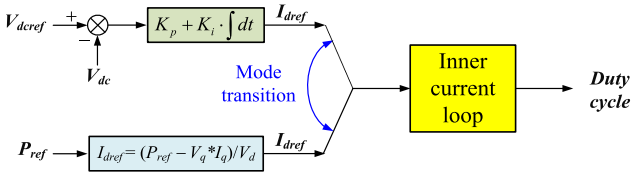

Fig. 13. Control block diagrams of $V_{\rm dc}/Q$ and P/Q modes.

1) VSC 1 active power ramps to -0.8 p.u.;
2) VSC 1 active power ramps from – 0.8 to 0.8 p.u.;
3)VSC 2 reactive power ramps to 0.4 p.u.; and
4) VSC 4 active power ramps to – 0.8 p.u. As shown in Fig. 11, VSC 3 adjusts its active power to achieve the power balance in the dc grid, and the dc voltages are maintained well during all transients.

2) Voltage Droop Control: VSC 3 and 4 are changed to $V_{\rm dc} - P$ droop modes while VSC 1 and 2 remain in P/Q mode. The tested transients are almost the same as above except for step IV. With droop control, VSC 4 is not able to change the active power generation directly. Compared to the above case with voltage margin control, VSC 3 and 4 both adjust their active power to balance the system as shown in Fig. 12. The droop control lets the two converters share the responsibility for power balance.

The test results show that the dc voltages are maintained well for both methods. Therefore, the preference of voltage margin or droop control mainly depends on the system power dispatch requirement.

D. System Online Mode Transition

More than one control mode is usually deployed in each station. In the testbed, four control modes are implemented, which are $V_{\rm dc}$ control, P control, $V_{\rm dc} - P$ droop, and $P - V_{\rm dc}$ droop. There could be the need to change converter operation mode according to different power dispatch requirements, and it is much preferred not to require shutdown and restart of the converter during the mode transition. Therefore, converter online mode transition is required.

Fig. 13 shows the simplified block diagrams for $V_{\rm dc}$ and P control. Transition from P control to $V_{\rm dc}$ control can be realized through the following steps: 1) overwrite the integrator in $V_{\rm dc}$ control by the current d-axis current reference ($I_{d\,\rm ref}$), and the dc voltage reference ($V_{\rm dc\,ref}$) uses the currently measured dc voltage as the initial value; and 2) ramp the $V_{\rm dc\,ref}$ to its target value. This ensures no abrupt $I_{d\,\rm ref}$ transient during the mode transition. The transition from $V_{\rm dc}$ control to P control is similar, and even simpler as P control is an open loop. It is fulfilled by overwriting the active power reference ($P_{\rm ref}$) by the currently measured P, and then ramps $P_{\rm ref}$ to the target value.

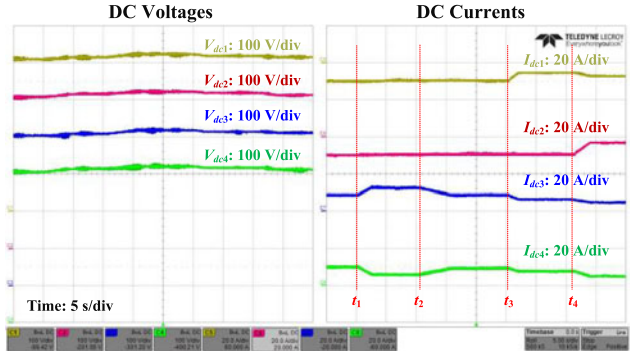

Fig. 14. Waveforms of station online mode transition.

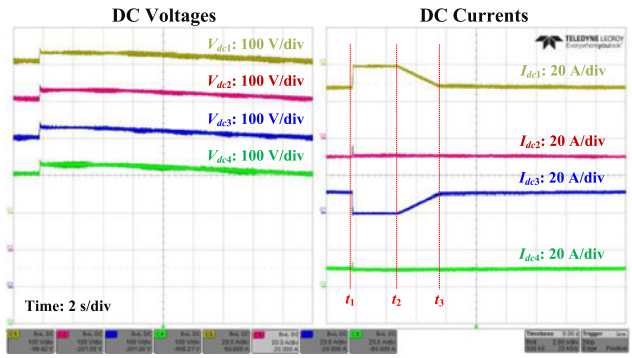

Fig. 15. Waveforms of VSC 3 failure with voltage margin control.

Fig. 14 shows the test result including different mode transitions. Originally, VSC 3 operates at $V_{\rm dc}$ control mode and the rest of the converters are at P control mode. VSC 4 and VSC 3 change to $V_{\rm dc} - P$ droop mode at t_1 and t_2, respectively. VSC 1 and VSC 2 then change to $P - V_{\rm dc}$ droop mode at t_3 and t_4, respectively. As shown in the waveform, the dc voltages are controlled well during all transitions, and dc currents change smoothly.

E. Station Failure

Under some circumstances the station may lose its power transfer capability, like during ac-side three-phase short circuit fault or some internal faults. The worst-case scenario is when this happens to a system voltage regulator. As mentioned in Section II, coordinated dc voltage control is needed to make sure at least one other station will automatically take over the voltage regulation responsibility, to avoid system collapse. This scenario has been tested for systems with voltage margin and droop control, respectively.

1) Voltage Margin Control: The test result is shown in Fig. 15. The VSC 3, which is normally controlling the dc voltage, is blocked at t_1. The dc voltage increases quickly and reaches the voltage limit of VSC 1. Then VSC 1 changes to $V_{\rm dc}$ control mode

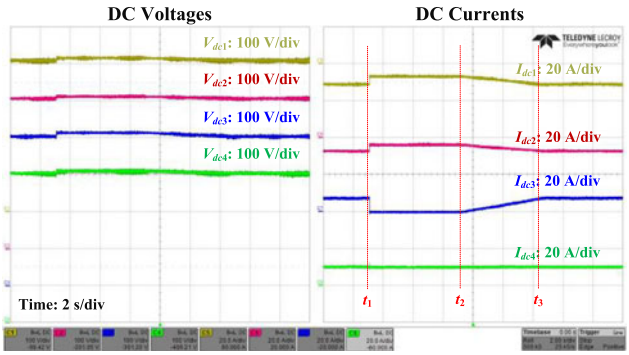

Fig. 16. Waveforms of VSC 3 failure with voltage droop control.

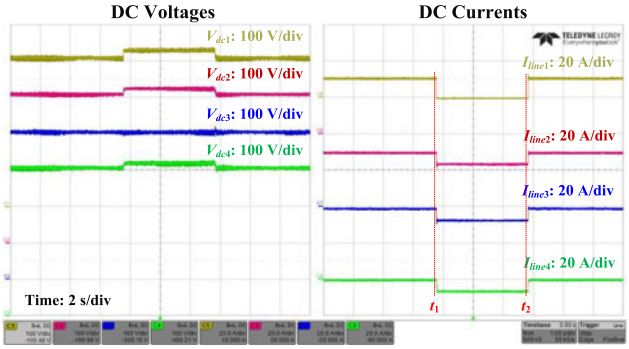

Fig. 17. Waveform of dc line disconnection and reconnection.

and starts to regulate the dc voltage. The active power of VSC 1 is immediately reduced for power balance. As shown in the waveform, the dc voltage can be controlled well. At t_2, VSC 3 is recommissioned. Similar to the mode transition, the initial dc voltage reference of VSC 3 is set equal to the measured dc voltage, and then slowly decreases to the target value. At t_3, VSC 1 goes back to P control mode and the dc voltage starts to decrease. Thus, the station recommission is very smooth with the voltage margin control.

2) Voltage Droop Control: To better demonstrate the effectiveness of droop control, the operating modes of VSC 1 and 2 are set to $P - V_{\rm dc}$ modes; VSC 3 operates in $V_{\rm dc}/Q$ mode and VSC 4 in P/Q mode. The test process is the same as that in the voltage margin case. As shown in Fig. 16, when VSC 3 is blocked, VSC 1 and 2 together take over the voltage control responsibility and share the active power reduction. The system performs well for this scenario. Again, the voltage margin and droop control do not differ much in terms of station failure scenario.

IV. DC Line Current Control and Limiting Function

A. DC Line Disconnection and Reconnection

If dc circuit breakers are installed in the MTDC system, dc lines can be online disconnected and reconnected for maintenance purposes or under situations like dc line short circuit fault. In the testbed, circuit breakers are installed at each terminal of the cable. Fig. 17 shows the test results of disconnecting cable 2 at t_1 and reconnecting it at t_2. The terminal dc voltages (excluding VSC 3) vary a little after cable 2 is removed, due to the dc system power flow change. No obvious current overshoot is observed during the disconnection and reconnection processes. However, it could occur depending on the system parameters, as this transient is a step change between two different dc grid configurations. The overshoot current should not be a concern for the cable due to the short time duration, but its impact on current protection design should be considered in order to avoid false tripping.

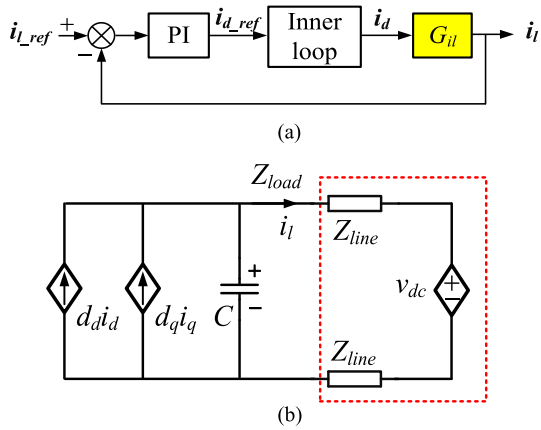

Fig. 18. DC line current control principle. (a) Block diagram and (b) average model of two-station setup.

B. DC Line Current Control

Since a cost-effective HVDC circuit breaker is still not available in the market, dc disconnects are more likely installed in the real system. Compared with the circuit breaker, the HVDC disconnect has very limited current blocking capability, for example, 200 A for a commercial product in [26]. Even though the disconnect cannot replace the circuit breaker for interrupting large fault current, it is still desirable if the disconnect can be used for online disconnection of the line for maintenance purposes, without de-energizing the entire system. Due to the small current blocking capability of the disconnect, only the line with very little current can be online disconnected. A dc line current control is, therefore, proposed. The line current will be first controlled to be small, and then get disconnected.

As line current depends on the line impedance and voltage difference between the two terminals, it can be controlled by terminal voltage of either connected station. Fig. 18(a) shows a simplified block diagram of the proposed dc line current control in one station (i_l and $i_{\rm lref}$ represent the line current and its reference value). It is similar to dc voltage regulator, except that the dc line current loop becomes the outer loop. The inner loop ($i_d/i_{d\ \rm ref}$) is the same, which is simplified as one block in the figure. For the controller design, the key is to find the transfer function ($G_{\rm il}$) between i_l and i_d. Fig. 18(b) shows the average model in *dq* coordinates [27] for a two-terminal system by considering the other converter as an ideal voltage regulator, and d_d, d_q in the figure are the duty cycles in *d*-axis and *q*-axis,

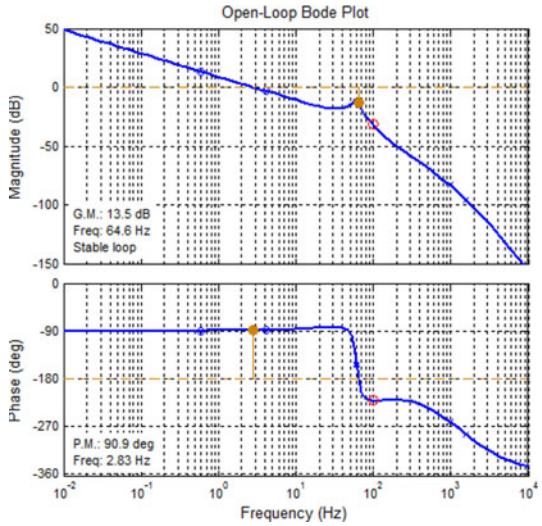

Fig. 19. Bode plot of the dc line current control with the designed compensator.

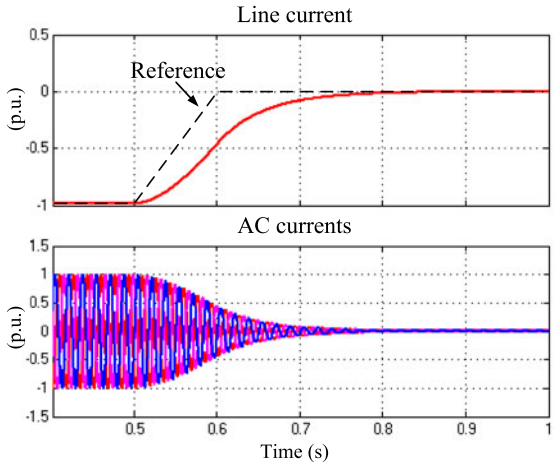

Fig. 20. Simulation results on a two-terminal system.

respectively. The transfer function $G_{\rm il}$ is derived as follows:

$$G_{\rm il} = \frac{D_d}{Z_{\rm load}/Z_c + 1} \tag{1}$$

where $Z_{\rm load}$ is the equivalent load impedance including line impedance and voltage regulator impedance. Z_c is the dc-link capacitor impedance. With the transfer function, the dc line current controller can be designed. For the multiterminal case, the only difference is the equivalent load impedance. However, the modeling of the multiterminal system is more complicated [28], which will not be covered in this paper.

Fig. 19 shows the open-loop bode plot of the dc line control in a two-terminal system with the designed compensator. There exists a resonance peak due to the line inductor and dc capacitor, and the bandwidth is thus relatively low.

Fig. 20 shows the simulation waveform for a two-terminal system. The line current control is first disabled. At 0.5 s, the converter switches from active power control to dc line current control. The current reference ramps from the value at 0.5 s to zero in order to achieve a smooth control mode transition. The line current cannot follow the reference well due to the low control bandwidth, but will go to zero eventually.

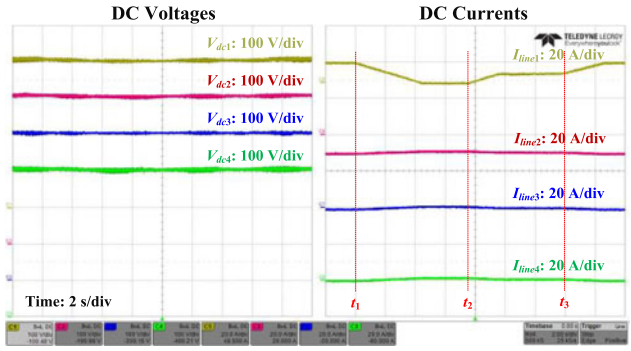

Fig. 21. Waveforms of dc line current control.

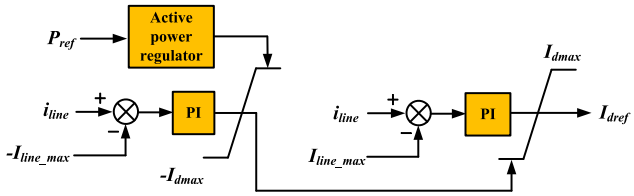

Fig. 22. Implementation of dc line current limiting scheme.

Fig. 21 shows the test result by implementing the line current control in line 1. At t_1, the line current control is enabled and the reference current is zero. The current of line 1 ramps to zero, while the currents of the remaining lines stay almost the same. At t_2, the reference current is set to 5 A. The waveform shows the line current tracks the reference well. At t_3, the line current control is disabled and the line 1 current goes back to normal. As shown in Fig. 21, the line 1 current is controlled well and has little impact on other lines. The dc voltage control will not be impacted either.

With the dc line current control, transmission line online disconnection can be achieved by using the low-cost HVDC disconnect. However, it cannot be used for faulted line isolation during a dc short circuit fault. For dc fault protection, either an ac circuit breaker [29] or a fault tolerant converter [30] should be used to break or control the fault current, and then use the dc disconnect to isolate the faulted line. The other option is to replace the dc disconnect with a dc circuit breaker. The hybrid dc circuit breaker [8] is mostly considered due to its good performance balance between fast speed [31] and low operation loss. But practically due to the high cost, it may not be installed in every transmission line. So the proposed control can still be useful for lines without the hybrid dc circuit breakers.

C. DC Line Current Limiting Function

Utilizing the proposed dc line current control, another idea is proposed for current limiting if the line is overloaded. The concept is as follows: when the line current becomes larger than the allowed maximum value, the line current control is "enabled" and regulates the current at the maximum value. If

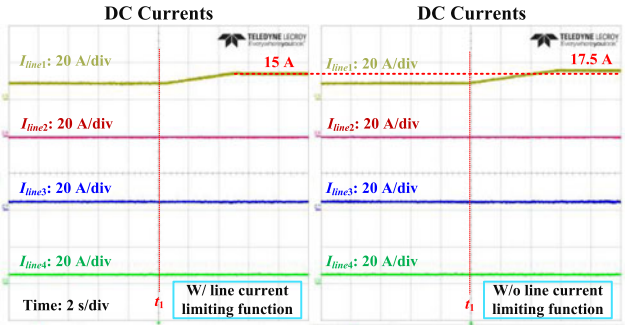

Fig. 23. Waveform of dc line current limiting function test.

the line current goes back to the normal region, the line current control is automatically "disabled." The implementation of this line current limiting scheme is shown in Fig. 22, which is similar to the voltage margin control. Two line current regulators are applied with the reference currents equal to the positive and negative maximum allowed line current, respectively. Normally, if the line current is within the maximum value, both the line current regulators are saturated, and $I_{d\,\mathrm{ref}}$ is generated by the active power regulator. But if the line is overloaded, one of the line current regulators will be desaturated and limit the current at either the positive or negative maximum value.

Fig. 23 shows an experimental test result by implementing the line current limiting function. The left side waveform is with line current limiting function at a maximum current of 15 A, and the right side waveform is without line current limiting function. At t_1, the active power of VSC 1 is increased and the line 1 current starts increasing. For the case without the limiting function, the line 1 current goes as high as 17.5 A; while with the limiting function, the current only reaches 15 A, which means the line current control becomes active.

V. Conclusion

A four-terminal down-scaled HVDC testbed is developed, corresponding to a hypothetical system proposed for transferring power from two offshore wind farms to two onshore load centers. The developed testbed is capable of emulating some typical operation scenarios, including system start-up, power variation, line contingency, and converter station failure. The two most popular coordinated dc voltage controls – voltage margin and voltage droop, have been implemented and tested. The test results verify their capability to regulate dc voltage well in different conditions and also reveal that their main difference is the system power dispatch. This paper also demonstrates two unique scenarios, station online recommission, and mode transition. For station online recommission, a new method is proposed and compared with an existing method. The proposed one has the benefit of easy implementation, but will cause system power flow change as well as the inrush current which flows through the power devices in the converter. Fortunately, the inrush current can be limited by the voltage margin control.

In addition, a dc line current control is proposed and verified through experiment. Two benefits associated with this control have been explained in the paper. First, it facilitates the use of low-cost HVDC disconnect to open a dc transmission line. Second, it can be used to realize dc line current limiting function, which helps to prevent dc line overloading.

References

[1] U.S. Department of Energy. (2013). Wind vision: A new era for wind power in the United States [Online]. Available: http://www.energy.gov
[2] Siemens. High voltage direct current transmission – proven technology for power exchange [Online]. Available: http://www.siemens.com
[3] N. Flourentzou, V. G. Agelidis, and G. D. Demetriades, "VSC-based HVDC power transmission systems: An overview," *IEEE Trans. Power Electron.*, vol. 24, no. 3, pp. 592–602, Mar. 2009.
[4] ABB. (2013). It's time to connect with offshore wind supplement [Online]. Available: http://www.abb.com/hvdc
[5] P. L. Francos, S. S. Verdugo, H. F. Álvarez, S. Guyomarch, and J. Loncle, "INELFE—Europe's first integrated onshore HVDC interconnection," in *Proc. IEEE Power Energy Soc. Gen. Meeting*, 2012, pp. 1–8.
[6] G. Asplund, K. Linden, C. Barker, A. Marzin, U. Baur, N. Pahalawaththa, J. Beerten, M. Rashwan, P. Christensen, J. Rittiger, S. Cole, K. Sogaard, D. Van Hertem, D. Westermann, J. Wen, E.-D. Wilkening, D. Jovcic, C. Yue, and P. Labra, "HVDC grid feasibility study," Working Group B4-52, CIGRE, *Paris, France*, 2013.
[7] Twenties project report. (2013). Comparison of different network solutions in the North Sea offshore system [Online]. Available: http://twenties-project.eu
[8] J. Hafner and B. Jacobson, "Proactive hybrid HVDC breakers – A key innovation for reliable HVDC grids," in *Proc. CIGRE Symp.*, *Bologna, Italy*, 2011.
[9] Twenties project report. (2014). Test results of DC breaker demonstrator addendum to deliverable [Online]. Available: http://twenties-project.eu
[10] R. Wachal, A. Jindal, S. Dennetiere, H. Saad, O. Rui, S. Cole, M. Barnes, L. Zhang, Z. Song, J. Jardini, J. C. Garcia, F. Mosallat, H. Suriyaarachich, P. Le-Huy, A. Totterdell, L. Zeni, S. Kodsi, T. Deepak, P. Thepparat, T. Beddard, J. Velasquez, S. D'Arco, A. Morales, Y. Kono, T. K. Vrana, and Y. Yang, "Guide for the development of models for HVDC converters in a HVDC grid," Working Group B4-57, CIGRE, *Paris, France*, 2014.
[11] K. Sharifabadi, P. Adam, M. Ferraz, S. Achenbach, B. Andersen, A. Benchaib, A. D. Castro, C. Higgins, P. Holmberg, V. Hussennether, A. Khan, P. Labra, A. Marzin, T. Miles, R. H. Renner, C. Smith, and D. V. Hertem, "Guidelines for the preparation of 'connection agreements'or 'grid codes' for multi-terminal DC schemes and DC grids," Working Group B4-56, CIGRE, *Paris, France*, 2016.
[12] H. Rao, "Architecture of Nan'ao multi-terminal VSC-HVDC system and its multi-functional control," *CSEE J. Power Energy Syst.*, vol. 1, no. 1, pp. 9–18, Mar. 2015.
[13] G. Tang, Z. He, H. Pang, X. Huang, and X. Zhang, "Basic topology and key devices of the five-terminal dc grid," *CSEE J. Power Energy Syst.*, vol. 1, no. 2, pp. 22–35, Jun. 2015.
[14] Y. Li, X. Shi, B. Liu, F. Wang, L. M. Tolbert, and W. Lei, "Hardware implementation of a four-terminal HVDC test-bed," in *Proc. IEEE Energy Convers. Congr. Expo.*, 2015, pp. 5363–5370.
[15] A. Alvarez, F. Bianchi, A. Ferre, G. Gross, and O. Bellmunt, "Voltage control of multiterminal VSC-HVDC transmission systems for offshore wind power plants: design and implementation in a scaled platform," *IEEE Trans. Ind. Electron.*, vol. 60, no. 6, pp. 2381–2391, Jun. 2013.
[16] Twenties project report. (2013). Testing results from DC network mock-up and DC breaker prototype [Online]. Available: http://twenties-project.eu
[17] H. Stoylen, K. Uhlen, A. Ardal, and K. Sharifabadi, "Laboratory demonstration of an offshore grid in the North Sea with dc droop control," in *Proc. 9th Int. Conf. Ecological Veh. Renewable Energies*, 2014, pp. 1–8.
[18] S. Wang, C. D. Barker, R. S. Whitehouse, and J. Liang, "Experimental validation of autonomous converter control in a HVDC grid," in *Proc. Eur. Conf. Power Electron. Appl.*, 2014, pp. 1–10.
[19] D. Van Hertem, O. G. Bellmunt, and J. Liang, "HVDC grid layouts," in *HVDC Grids for Offshore and Supergrid of the Future*. Hoboken, NJ, USA: Wiley, 2016, ch. 8, sec. 2, pp. 172–175.
[20] Charles River Associates, "Update to the analysis of the impact of Cape Wind on lowering New England energy prices," (Mar. 2012). [Online]. Available: http://capewind.org/sites/default/files/downloads/CRA-Updated-Cape-Wind-Report-29Mar2012_0.pdf
[21] H. Saadat, "Line model and performance," in *Power System Analysis*, 3rd ed. New York, NY, USA: McGraw-Hill, 2010.

[22] T. Nakajima and S. Irokawa, "A control system for HVDC transmission by voltage source converters," in *Proc. IEEE Power Eng. Soc. Summer Meeting*, 1999, pp. 1113–1119.
[23] L. Xu and L. Yao, "Dc voltage control and power dispatch of a multi-terminal HVDC system for integrating large offshore wind farms," *IET Renewable Power Gen.*, vol. 5, no. 4, pp. 223–233, 2011.
[24] X. Li, Z. Yuan, J. Fu, Y. Wang, T. Liu, and Z. Zhu, "Nanao multi-terminal VSC-HVDC project for integrating large-scale wind generation," in *Proc. IEEE PES Gen. Meeting*, 2014, pp. 1–5.
[25] Trench. (2012). HVDC divider – compensated voltage divider for HVDC transmission system [Online]. Available: http://www.trenchgroup.com
[26] "ZGW6-816/J6300-25 high voltage dc disconnect switch" in Product list. [Online]. Available: http://www.pinggao.com/products_detail/productId=80.html
[27] S. Hiti, D. Boroyevich, and C. Cuadros, "Small-signal modeling and control of three-phase PWM converters," in *Proc. Ind. Appl. Soc. Annu. Meeting*, 1994, pp. 1143–1150, vol. 2.
[28] G. O. Kalcon, G. P. Adam, O. Lara, S. Lo, and K. Uhlen, "Small-signal stability analysis of multi-terminal VSC-based dc transmission systems," *IEEE Trans. Power Syst.*, vol. 27, no. 4, pp. 1818–1830, Nov. 2012.
[29] L. Tang, "Control and protection of multi-terminal dc transmission systems based on voltage-source converters," Ph.D. dissertation, ECE, McGill University, Montreal, QC, Canada, 2003.
[30] R. Marquardt, "Modular multilevel converter topologies with dc-short circuit current limitation," in *Proc. IEEE Int. Conf. Power Electron. ECCE Asia*, 2011, pp. 1425–1431.
[31] C. Peng, A. Q. Huang, I. Husain, B. Lequesne, and R. Briggs, "Drive circuits for ultra-fast and reliable actuation of Thomson coil actuators used in hybrid ac and dc circuit breakers," in *Proc. IEEE Appl. Power Electron. Conf.,* 2016, pp. 2927–2934.

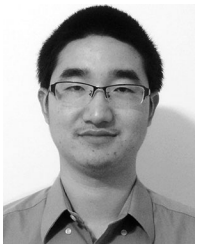

Yalong Li (S'12) received the B.S. degree from Huazhong University of Science and Technology, Wuhan, China, in 2011 and the M.S. degree from the University of Tennessee, Knoxville, TN, USA in electrical engineering, in 2013, where he is currently working toward the Ph.D. degree in electrical engineering.

He has been with Center for Ultra-wide-area Resilient Electric Energy Transmission Networks Research Center, University of Tennessee since 2011. His research interests include modular multilevel converters and high-voltage dc transmission.

Xiaojie Shi (S'11) received the M.S. degree from Zhejiang University, Hangzhou, China, in 2011, and the Ph.D. degree from the University of Tennessee, Knoxville, TN, USA, in 2015, both in electrical engineering.

She is currently a Research Assistant Professor at the Center for Ultra-wide-area Resilient Electric Energy Transmission Networks, University of Tennessee, Knoxville, TN, USA. Her research interests include microgrid, high-power grid-connected converters, HVDC transmission systems, and integration of distributed energy resources.

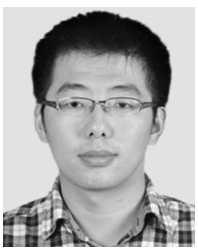

Bo Liu (S'11) received the B.S. and M.S. degrees in electrical engineering from Xi'an Jiaotong University, Xi'an, China, in 2009 and 2012, respectively. He is currently working toward the Ph.D. degree in electrical engineering at the Center for Ultra-wide-area Resilient Electric Energy Transmission Networks, University of Tennessee, Knoxville, TN, USA.

His current research interests include hybrid ac/dc transmission system, grid emulation, GaN-based high-frequency high-density three-phase rectifier, and conducted electromagnetic interference.

Wanjun Lei (S'06–M'09) was born in Shannxi, China, in 1978. He received the B.S., M.S., and Ph.D. degrees from the School of Electrical Engineering, Xi'an Jiaotong University, Xi'an, China, in 2000, 2004, and 2008, respectively.

He is currently an Assistant Professor of electrical engineering at Xi'an Jiaotong University. He has published more than 20 journal and conference articles and holds several authorized China and U.S. patents in these areas. His research interests include power quality control, active distribution technical and flexible transmission.

Dr. Lei received the 2011 National Scientific and Technological Awards of China and the 2008 Scientific and Technological Awards from Shaanxi Province.

Fei (Fred) Wang (S'85-M'91-SM'99-F'10) received the B.S. degree from Xi'an Jiaotong University, Xi'an, China, and the M.S. and Ph.D. degrees from the University of Southern California, Los Angeles, CA, USA, in 1982, 1985, and 1990, respectively, all in electrical engineering.

He was a Research Scientist in the Electric Power Lab, University of Southern California, from 1990 to 1992. He joined the GE Power Systems Engineering Department, Schenectady, NY, USA, as an Application Engineer in 1992. From 1994 to 2000, he was a Senior Product Development Engineer with GE Industrial Systems, Salem, VA, USA. During 2000 to 2001, he was the Manager of Electronic & Photonic Systems Technology Lab, GE Global Research Center, Schenectady, NY and Shanghai, China. In 2001, he joined the Center for Power Electronics Systems at Virginia Tech, Blacksburg, VA as a Research Associate Professor and became an Associate Professor in 2004. From 2003 to 2009, he also served as the CPES Technical Director. Since 2009, he has been with The University of Tennessee and Oak Ridge National Lab, Knoxville, TN, USA, as a Professor and the Condra Chair of Excellence in Power Electronics. He is a founding member and the Technical Director of the multiuniversity NSF/DOE Engineering Research Center for Ultra-wide-area Resilient Electric Energy Transmission Networks led by the University of Tennessee, Knoxville, TN, USA. His research interests include power electronics, power systems, controls, electric machines, and motor drives.

Leon M. Tolbert (S'87–M'91–SM'97–F'13) received the Bachelor's, M.S., and Ph.D. degrees in electrical engineering from Georgia Tech, Atlanta, GA, USA, in 1989, 1991, and 1999, respectively.

He joined Oak Ridge National Laboratory (ORNL) in 1991 and worked on several electrical distribution projects at the three U.S. Department of Energy plants in Oak Ridge, TN, USA, from 1991 to 1999. He joined the University of Tennessee in 1999 and is currently the Min H. Kao Professor and the Department Head in Electrical Engineering and Computer Science. He is a founding member and thrust leader of CURENT, the NSF/DOE Engineering Research Center established at UT in 2011 to examine the structure and control of future electric grids. He is also a Part Time Senior Research Engineer at ORNL and conducts joint research in the Power Electronics and Electric Machinery Research Center. He does research in the areas of electric power conversion for renewable energy sources, multilevel converters, utility application of power electronics, microgrids, electric vehicles, and application of wide bandgap (SiC and GaN) power electronics.

Dr. Tolbert is a Registered Professional Engineer in the State of Tennessee. He was elected as a Member-at-Large to the IEEE Power Electronics Society Advisory Committee for 2010-2012, and has served as the Chair of the PELS Membership Committee and Education Committee. He was an Associate Editor of the IEEE TRANSACTIONS ON POWER ELECTRONICS from 2007 to 2012. He has been the Transactions Review Chair for the IEEE TRANSACTIONS ON INDUSTRY APPLICATIONS for the Industrial Power Converter Committee since 2014. He is the coauthor of six IEEE papers that have received prize paper awards.